Optimization of M_4 positive allosteric modulators (PAMs): The discovery of VU0476406, a non-human primate *in vivo* tool compound for translational pharmacology

Bruce J. Melancon, Michael R. Wood, Meredith J. Noetzel, Kellie D. Nance, Eileen M. Engelberg, Changho Han, Atin Lamsal, Sichen Chang, Hyekyung P. Cho, Frank W. Byers, Michael Bubser, Carrie K. Jones, Colleen M. Niswender, Michael W. Wood, Darren W. Engers, Dedong Wu, Nicholas J. Brandon, Mark E. Duggan, P. Jeffrey Conn, Thomas M. Bridges, Craig W. Lindsley

PII: S0960-894X(17)30421-3
DOI: http://dx.doi.org/10.1016/j.bmcl.2017.04.043
Reference: BMCL 24896

To appear in: *Bioorganic & Medicinal Chemistry Letters*

Received Date: 17 March 2017
Revised Date: 11 April 2017
Accepted Date: 12 April 2017

Please cite this article as: Melancon, B.J., Wood, M.R., Noetzel, M.J., Nance, K.D., Engelberg, E.M., Han, C., Lamsal, A., Chang, S., Cho, H.P., Byers, F.W., Bubser, M., Jones, C.K., Niswender, C.M., Wood, M.W., Engers, D.W., Wu, D., Brandon, N.J., Duggan, M.E., Jeffrey Conn, P., Bridges, T.M., Lindsley, C.W., Optimization of M_4 positive allosteric modulators (PAMs): The discovery of VU0476406, a non-human primate *in vivo* tool compound for translational pharmacology, *Bioorganic & Medicinal Chemistry Letters* (2017), doi: http://dx.doi.org/10.1016/j.bmcl.2017.04.043

Graphical Abstract

To create your abstract, type over the instructions in the template box below.
Fonts or abstract dimensions should not be changed or altered.9.0_/0

Optimization of M_4 positive allosteric modulators (PAMs): The discovery of VU0476406, a non-human primate *in vivo* tool compound for translational pharmacology

Leave this area blank for abstract info.

Bruce J. Melancon, Michael R. Wood, Meredith J. Noetzel, Kellie D. Nance, Eileen M. Engelberg, Changho Han, Atin Lamsal, Sichen Chang, Hyekyung P. Cho, Frank W. Byers, Michael Bubser, Carrie K. Jones, Colleen M. Niswender, Michael W. Wood, Darren W. Engers, Dedong Wu, Nicholas J. Brandon, Mark E. Duggan, P. Jeffrey Conn, Thomas M. Bridges and Craig W. Lindsley

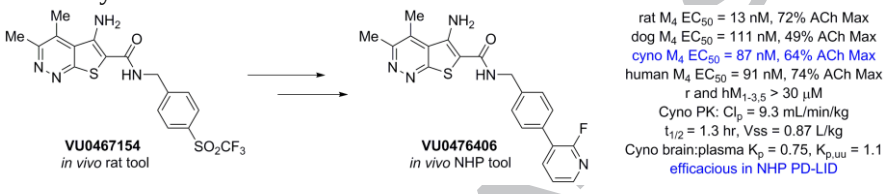

Bioorganic & Medicinal Chemistry Letters
journal homepage: www.elsevier.com

Optimization of M_4 positive allosteric modulators (PAMs): The discovery of VU0476406, a non-human primate *in vivo* tool compound for translational pharmacology

Bruce J. Melancon,[a,b] Michael R. Wood,[a,c] Meredith J. Noetzel,[a,b] Kellie D. Nance,[a] Eileen M. Engelberg,[a] Changho Han,[a] Atin Lamsal,[a] Sichen Chang,[a] Hyekyung P. Cho,[a,b] Frank W. Byers,[a] Michael Bubser,[a] Carrie K. Jones [a,b,e] Colleen M. Niswender,[a,b,e] Michael W. Wood,[d] Darren W. Engers,[a,b] Dedong Wu,[f] Nicholas J. Brandon,[d] Mark E. Duggan,[d] P. Jeffrey Conn,[a,b,e], Thomas M. Bridges [a,b*] and Craig W. Lindsley [a,b,c*]

[a]*Vanderbilt Center for Neuroscience Drug Discovery, Vanderbilt University Medical Center, Nashville, TN 37232, USA*
[b]*Department of Pharmacology, Vanderbilt University School of Medicine, Nashville, TN 37232, USA*
[c]*Department of Chemistry, Vanderbilt University, Nashville, TN 37232, USA*
[d] *AstraZeneca, Neuroscience, Innovative Medicines & Early Development, Waltham, Massachusetts 02451 USA*
[e]*Vanderbilt Kennedy Center, Vanderbilt University School of Medicine, Nashville, TN 37232, USA*
[f]*AstraZeneca, Pharmaceutical Science, 35 Gatehouse Drive, Waltham, MA 02451, USA.*

**To whom correspondence should be addressed: thomas.m.bridges@vanderbilt.edu and craig.lindsley@vanderbilt.edu*

ARTICLE INFO

Article history:
Received
Revised
Accepted
Available online

Keywords:
M_4
Muscarinic acetylcholine receptor
Positive allosteric modulator (PAM)
Non-human primate (NHP)
Structure-Activity Relationship (SAR)

ABSTRACT

This letter describes the further chemical optimization of the 5-amino-thieno[2,3-*c*]pyridazine series (VU0467154/VU0467485) of M_4 positive allosteric modulators (PAMs), developed via iterative parallel synthesis, culminating in the discovery of the non-human primate (NHP) *in vivo* tool compound, VU0476406 (**8p**). VU0476406 is an important *in vivo* tool compound to enable translation of pharmacodynamics from rodent to NHP, and while data related to a Parkinson's disease model has been reported with **8p**, this is the first disclosure of the optimization and discovery of VU0476406, as well as detailed pharmacology and DMPK properties.

Muscarinic acetylcholine receptor subtype 4 (M_4) positive allosteric modulators (PAMs) represent a fundamentally new approach to treat multiple symptom domains of schizophrenia, Huntington's disease and Parkinson's disease (PD).[1-12] M_4 PAMs (**Figure 1**) represent the extreme of allosteric modulator caveats in terms of steep SAR, species differences in pharmacology (rat versus human versus cynomolgus (cyno) monkey versus dog M_4 PAM potency, affinity/cooperativity and subtype selectivity), poor solubility, and/or low CNS penetration.[3,10-16] Work in this area has been challenging since the first report by Eli Lilly of **1**, a human-preferring M_4 PAM.[1] Subsequent optimization efforts afforded **2**, which provided the first *in vivo* proof-of-concept (POC) for selective M_4 potentiation of endogenous acetylcholine in reversing amphetamine-induced hyperlocomotion (AHL) in rats.[3] Further efforts improved physiochemical/DMPK properties and delivered the *in vivo* rodent POC tool compound, **3**.[11,15] Finally, **4** afforded a balance in M_4 PAM activity across species, and was evaluated in depth as our first potential M_4 PAM clinical candidate.[16] Despite these advances, we required an *in vivo* non-

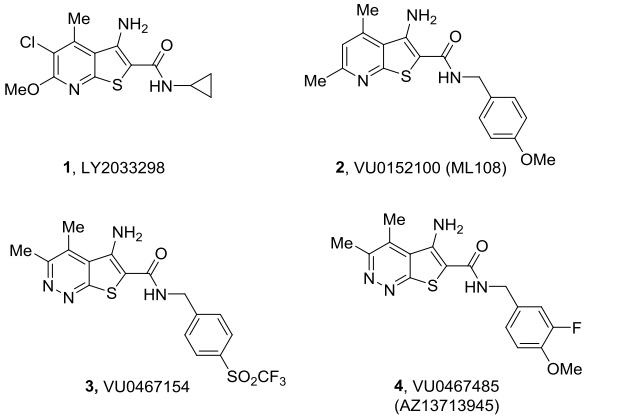

Figure 1. Structures of representative M_4 PAMs **1**-**4**, exemplifying an optimized rodent *in vivo* tool M_4 PAM, VU0467154 (**3**) and the clinical candidate VU0467485/AZ13713945 (**4**).

human primate (NHP) POC tool compound for use in translational efficacy studies, primate PD models and biomarker studies that could be freely shared with collaborators. In this Letter, we detail the discovery effort that led to VU0467406, an *in vivo* M_4 PAM non-human primate (NHP) tool compound.

As **4** offered balanced M_4 PAM activity across species, we focused our efforts on this chemotype.[16] A multitude of substituted benzyl amides had previously been explored, and SAR suggested a large lipophilic binding pocket accessible to the 4-position substituent, e.g., the 4-SO_2CF_3 moiety of **3** and related analogs. Interestingly, and despite their prevalence in GPCR ligands, we never synthesized and evaluated any biaryl or heterobiaryl methyl amide congeners; therefore, we focused our search for an NHP *in vivo* tool within this unexplored chemical space.

The synthesis of analogs **8** proved to be straightforward. Condensation of commercially available 3-chloro-5,6-dimethylpyridazine-4-carbonitrile **5** with methyl thioglycolate under basic conditions smoothly affords the sodium carboxylate **6** in 78% yield. A HATU-mediated amide coupling with 2-, 3- or 4-bromobenzyl amines then delivers analogs **7** in yields ranging from 45-92%. A subsequent Stille or Suzuki cross-coupling reaction with a diverse range of aryl and heteroaryl moieties delivers analogs **8** in yields ranging from 58-90%.[17]

Scheme 1. Synthesis of M_4 PAM analogs **8**.[a]

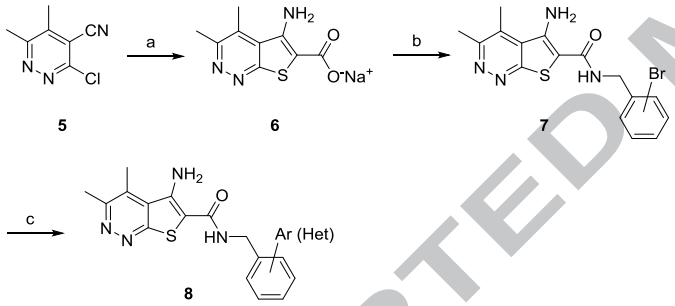

[a]Reagents and conditions: (a) Methyl thioglycolate, MeOH, 1M aq. NaOH, 150 °C, microwave, 30 min, 78%; (b) bromobenzyl amine, HATU, DMF, DIPEA, 2 h, 45-92%; (c) 5 mol% $Pd(dppf)Cl_2{\cdot}CH_2Cl_2$, $Bu_3SnAr(Het)$, THF, 65-80% or 5 mol% $Pd(dppf)Cl_2{\cdot}CH_2Cl_2$, $(HO)_2BAr(Het)$, K_3PO_4, THF/H_2O, 100 °C, 58-90%.

SAR was driven using activity at the human M_4 receptor (potency in functional assay), but key compounds were assessed on rat and cyno M_4 as well, as the goal was an NHP tool compound. As shown in **Table 1**, many potent human M_4 PAMs were discovered and several displayed attractive DMPK profiles and excellent CNS penetration (brain:plasma K_p and $K_{p,uu}$) *vide infra*. Initial evaluation of the 2-, 3- and 4-bromobenzyl derivatives, **7a-c** respectively, demonstrated a clear preference for 3- and 4- substitution. Conversion of these into the corresponding biaryl analogs, **8a-c,** confirmed the finding, with the 2-phenyl derivative **8a** inactive (hM_4 EC_{50} >10 μM), the 3-phenyl congener **8b** weak (hM_4 EC_{50} = 1.65 μM) while the 4-phenyl derivative **8c** displayed good M_4 PAM activity (hM_4 EC_{50} = 319 nM). Thus, future efforts focused solely on 4-substituted biaryl and heterobiaryl analogs **8d-p**. PAM **8c** showed low efficacy and poor physiochemical properties and a high cLogP (>4); therefore, we elected to evaluate diverse azaheterocycles in an attempt to improve physiochemical properties, enable salt formation and lower lipophilicity. Exploration of the pyridyl biaryl analogs **8d-f** showed robust SAR. Potency increased as the pyridine nitrogen was moved from the 2-position (**8d**, hM_4 EC_{50} = 232 nM), to the 3-position (**8e**, hM_4 EC_{50} = 103 nM) and finally to the 4-position (**8f**, hM_4 EC_{50} = 36 nM). Other heterocycles such as pyridazine (**8g**), pyrazine (**8h**), pyrimidine (**8i** and **8j**) were also well tolerated. Attempts to modulate the pyridine basicity in **8d-f** by the incorporation of fluorine atoms, as in **8k-p**, afforded a broad spectrum of activity, with **8k**, **8m** and **8p** displaying good hM_4 PAM potency and efficacy. From these initial analogs, PAMs **8f**, **8k**, **8m** and **8p** were selected for more in-depth DMPK profiling.

Table 1. Structures and activities for human M_4 PAM analogs **7 and 8.**

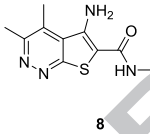

8

Cpd	R	hM_4 EC_{50} (nM)[a] [% ACh Max ±SEM]	hM_4 pEC_{50} (±SEM)
7a		>10,000 [31±2]	>5
7b		185 [84±2]	6.77±0.13
7c	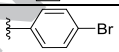	187 [82±2]	6.74±0.07
8a		>10,000 [30±1]	>5
8b	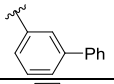	1,650 [41±3]	5.80±0.12
8c	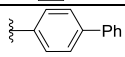	319 [49±6]	6.53±0.12
8d	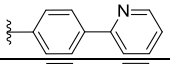	232 [75±5]	6.67±0.12
8e	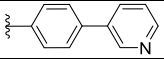	103 [63±4]	7.20±0.31
8f	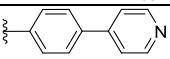	36 [83±8]	7.57±0.19
8g	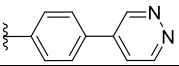	56 [96±5]	7.26±0.06
8h	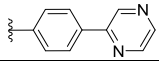	159 [63±6]	7.00±0.29
8i	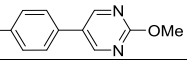	84 [91±9]	7.08±0.04
8j	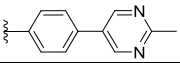	230 [65±11]	6.67±0.11
8k	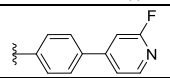	58 [92±10]	7.31±0.16
8l	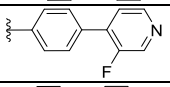	1,716 [86±5]	5.81±0.14
8m	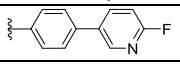	64 [79±2]	7.20±0.06
8n	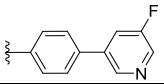	144 [78±14]	6.84±0.04
8o	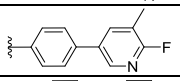	994 [68±1]	6.11±0.22
8p	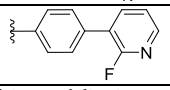	91 [74±3]	7.04±0.11

[a]Calcium mobilization assays with $hM_{4/Gqi5}$-CHO cells performed in the presence of an EC_{20} fixed concentration of acetylcholine; values represent means from three (*n*=3) independent experiments performed in triplicate.

As shown in **Table 2**, all four PAMs showed attractive cLogPs (2.66 to 2.92) and conserved TPSAs with molecular

weights below 500. All were highly bound in plasma, except **8f**, which also showed low rat clearance *in vivo* (despite high *in vitro* predicted rat CL_{hep}, a likely consequence of excluding fu_{plasma}/fu_{mic} terms from the well-stirred equation used for prediction) and high rat CNS penetration (brain:plasma K_p = 0.94, $K_{p,uu}$ = 1.1). However, **8f**, as expected due to the naked pyridine ring, was a potent inhibitor of multiple CYP_{450}s (IC_{50}s < 10 μM), including 3A4 (IC_{50} = 340 nM). Similarly, both **8k** and **8m** were potent inhibitors of 1A2 (IC_{50}s of 2.5 μM and 790 nM, respectively) with low rat *in vivo* clearance (CL_ps of 3.6 and 1.7 mL/min/kg, respectively) and moderate total brain distribution (K_ps <0.21). Here, **8p** stood out, with an improved CYP inhibition profile (all IC_{50}s ≥11 μM) andfavorable rat PK (CL_p = 1.6 mL/min/kg, elim. $t_{1/2}$ = 2.7 hr) despite a moderate K_p (0.11), an attractive $K_{p,uu}$ (1.2). Moreover, **8p** was not a human P-gp substrate *in vitro* (ER = 1.7). However, we noted a lack of an *in vitro/in vivo* correlation (IVIVC) between the *in vitro* predicted CL_{hep} and the *in vivo* CL_p. Employing a revised prediction method (inclusion of binding terms in the well-stirred model), the predicted rat CL_{hep} decreased to 0.49 mL/min/kg, and a more robust IVIVC resulted.

Table 2. *In vitro* and *in vivo* DMPK properties of **8f**, **8k**, **8m** and **8p**.

Property	**8f**	**8k**	**8m**	**8p**
MW	398.4	407.4	407.4	407.4
cLogP	2.66	2.92	2.92	2.92
TPSA	93.4	93.8	93.8	93.8
In vitro PK parameters				
CL_{INT} (mL/min/kg), rat	415	57.1	81.6	134.0
CL_{HEP} (mL/min/kg), rat	59.9	31.5	37.7	46.0
CL_{INT} (mL/min/kg), human	20.1	19.6	20.2	19.2
CL_{HEP} (mL/min/kg), human	15.2	17.8	17.1	14.8
Rat fu_{plasma}	0.037	0.002	0.004	0.002
Human fu_{plasma}	0.013	0.029	0.023	0.011
Rat fu_{brain}	0.042	ND	ND	0.020
Cytochrome P_{450} (IC_{50}, μM)				
1A2	9.7	2.5	0.79	11
2C9	2.3	25	26	>30
2D6	1.3	>30	>30	19
3A4	0.34	24	25	>30
IV Pharmacokinetics (SD Rat; 0.1-1.0 mg/kg)				
CL_p (mL/min/kg)	9.0	3.6	1.7	1.6
Elimination t½ (hr)	1.5	1.7	0.48	2.7
V_{ss} (L/kg)	1.1	0.50	0.60	0.34
Brain Distribution (0.25 hr) (SD Rat; 0.1-0.2 mg/kg IV)				
$K_{p,\ brain:plasma}$	0.94	0.21	0.13	0.11
$K_{p,uu,\ brain:plasm}$	1.1	ND	ND	1.2
MDCK-MDR1 (Pgp) ER	1.1	ND	ND	1.7

ND = not determined.

While **8p** emerged as the most attractive of the analogs of **8** that were surveyed, we wanted to explore modifications to the benzylic phenyl ring before initiating a more exhaustive profiling effort around **8p**. While many analogs in which fluorine atoms and/or nitrogen atoms were added retained excellent M_4 PAM potency (EC_{50}s < 200 nM), all suffered from increased cLogP, poor *in vitro*/*in vivo* clearance and/or unacceptable CYP inhibition profiles. Thus, **8p** was advanced as a potential NHP tool compound.

Next, **8p** was evaluated as an M_4 PAM across multiple species (**Figure 2**). Unlike all predecessors (except **4**), **8p** was a potent M_4 PAM at the rat (rM_4 EC_{50} = 13.5 nM, pEC_{50} = 7.93±0.17, 72±4% ACh Max), human (hM_4 EC_{50} = 91.0 nM, pEC_{50} = 7.04±0.11, 74±3% ACh Max), dog (dM_4 EC_{50} = 111 nM, pEC_{50} = 6.95±0.12, 49±4% ACh Max) and cyno receptors (cM_4 EC_{50} = 87.3 nM, pEC_{50} = 7.06±0.25, 64±2% ACh Max). ACh concentration response curve (CRC) fold-shift Ca^{2+} mobilization and ACh competition binding (with [^{3}H-*N*-methylscopolamine) assays provided operational model parameters for **8p** at rM_4 (K_B = 0.37 μM, α = 8.4, β = 9.1),hM_4 (K_B = 2.8 μM, α = 7.0, β = 21), and cyno M_4 (K_B= 2.1 μM, α=28.2, β=2.5); all experiments are n=3-4, performed in duplicate. Moreover, **8p** was inactive (EC_{50} > 30 μM) at both rat and human $M_{1\text{-}3,5}$ (and also inactive at dog and cyno M_2, data not shown). These data were highly noteworthy and indicated that **8p** was a potent and highly-selective NHP M_4 PAM. A broad secondary pharmacology panel (Cerep) revealed only one sub-micromolar off-target activity for **8p** – a rat $GABA_A$ receptor (benzodiazepine site) binding IC_{50} = 0.44 μM, which was subsequently de-risked by a functional assay determination (no activity at 10 μM). A functional electrophysiology hERG assay with **8p** was likewise clean (IC_{50} > 33 μM), and a mini-Ames assay (TA98 and TA100 strains ± S9) was negative for mutagenicity. In addition, **8p** was devoid of evidence for CYP 1A2/2B6/3A4 induction potential in cryopreserved human hepatocytes (48 hr incubation with enzyme activity readout; EC_{50}s > 50 μM, E_{max}s < 2), and in a 4 day sub-chronic dosing rat study (10 mg/kg, QD PO, *n* = 2), the day 4 versus day 1 $AUC_{0\text{-}\infty}$ ratio was 0.77, indicating little to no auto-induction *in vivo* in rat.

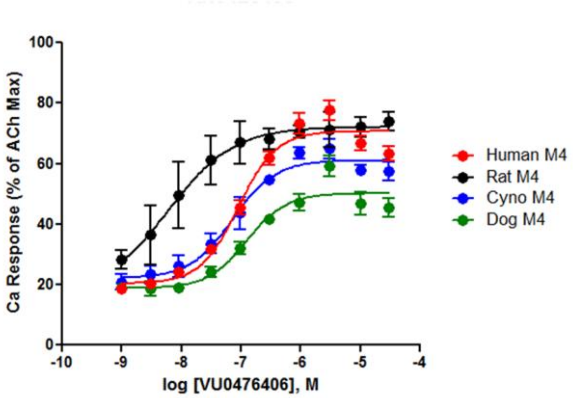

Figure 2. M_4 PAM concentration response curves (CRCs) for **8p** (VU0476406) at human (hM_4 EC_{50} = 91.0 nM, pEC_{50} = 7.04±0.11, 74±3% ACh Max), rat (rM_4 EC_{50} = 13.5 nM, pEC_{50} = 7.93±0.17, 72±4% ACh Max), cyno (cM_4 EC_{50} = 87.3 nM, pEC_{50} = 7.06±0.25, 64±2% ACh Max) and dog (dM_4 EC_{50} = 111 nM, pEC_{50} = 6.95±0.12, 49±4% ACh Max).

Compound **8p** was found to possess a largely attractive PK profile across species. In rat, **8p** as a 10 mg/kg solution dose achieved good oral bioavailability (61% F), and the HCl salt of **8p**, when dosed as a suspension, achieved 54 %F. PAM **8p** likewise exhibited favorable IV and PO PK in dog (CL_p = 5.5 mL/min/kg, elim. $t_{1/2}$ = 1.0 hour, V_{ss} = 0.70 L/kg, and 47 %F from 3 mg/kg suspension dose of the HCl salt) and favorable IV PK in cynomolgus monkey (CL_p = 9.3 mL/min/kg, elim. $t_{1/2}$ = 1.3 hours, V_{ss} = 0.87 L/kg), but with low oral bioavailability (4.7 %F from 10 mg/kg solution dose of HCl salt). CNS penetration of **8p** was also assessed in dog (brain:plasma K_p = 0.74, $K_{p,uu}$ = 2.6, C_{csf}:$C_{plasma,u}$ = 4.8 at 2.0 hr; via a terminal study) and NHP (brain:plasma K_p = 0.75, $K_{p,uu}$ = 1.1, C_{csf}:$C_{plasma,u}$ = 1.0 at 1 hr; via a PET study measuring brain distribution of [^{18}F]-VU0476406 after IV administration),[18] providing strong support for the utility of **8p** in NHP behavioral models and biomarker studies.

Encouraged, we performed additional studies to evaluate **8p** (VU0476406) as a potential candidate for clinical development before releasing it as a public M_4 PAM NHP tool compound. *In vitro* metabolite identification experiments employing

cryopreserved hepatocytes found low turnover and no evidence for human unique metabolites, with rat and cyno anticipated to provide adequate coverage of human metabolites (**Figure 3**). Human CYP_{450} phenotyping experiments revealed that multiple CYPs (3A4 (predominant), 2D6, 2C19, 2C9 and 1A2) contribute to **8p**'s metabolism. Moreover, no significant levels of GSH conjugates were observed in reactive metabolism/bioactivation experiments with human hepatic microsomes, which further bolstered the potential to advance **8p**.

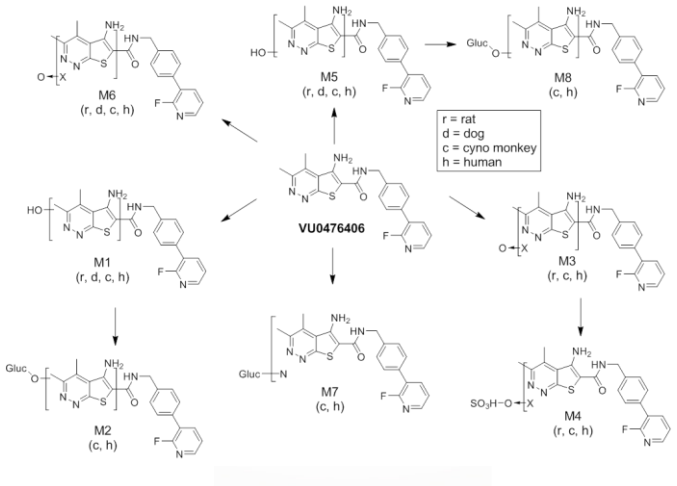

Figure 3. *In vitro* biotransformation of **8p** (VU0476406) in cryopreserved hepatocytes from multiple species (rat, dog, cynomolgus monkey, and human).

Human PK prediction, utilizing multiple approaches, suggested that **8p** would exhibit low clearance in man (CL_p between 1.3 to 3.6 mL/min/kg) with a 6-17 hour half-life.[19] However, for projected 12-hour daily coverage (targeting an efficacious C_{min} scaled from rat *in vivo* pharmacodynamic studies; data not shown), **8p** was projected to require moderate to high BID oral doses (370 - 850 mg) due in large part to moderate predicted human oral F. In parallel, pharmaceutical science work on both the free base and HCl salt was performed, which found **8p** to be highly crystalline with low aqueous solubility (< 0.5 µM for free base at pH 7.4) and without a clean melt (free base

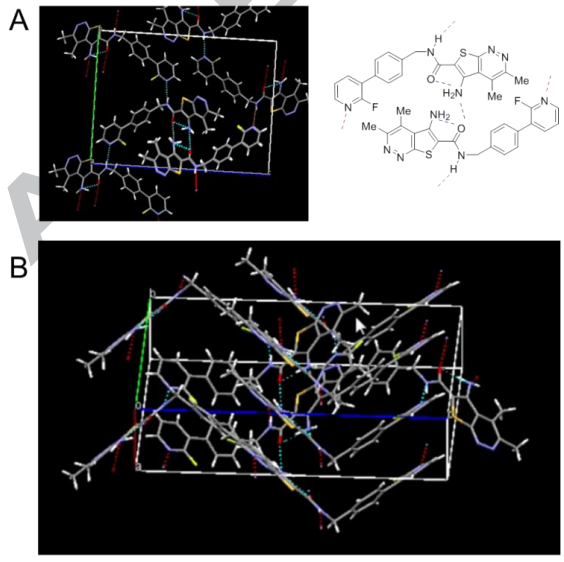

Figure 4. X-ray crystal structure (CCDC 1538487) of **8p**. A) Clear intra- and intermolecular hydrogen bonds are present (H-bond between pyridine and amide is linear, H-bond network forms a helix). B) All aryl/heteroaryl rings are oriented to allow π-stacking on both faces. Unit cell dimensions: 22.3 x 16.8 x 5.04 Å. Combined, this crystalline lattice explains the compound's poor aqueous solubility.

decomposes at 243-246 °C), suggesting potential challenges to achieving requisite margins in nonclinical safety and toxicology studies. An X-ray crystal structure proved telling (**Figure 4**), highlighting a network of intra- and inter-molecular hydrogen bonds forming a tight, helix-like packing with highly ordered π-stacking. Efforts to disrupt this network to enable acceptable solubility/dissolution with vehicles suitable for IND-enabling safety and toxicology studies were not successful. Thus, based on the suboptimal physiochemical properties of **8p** and the high projected human doses, the program team decided to release **8p** as a publicly available NHP M_4 PAM tool compound.

Upon release, Surmeier and co-workers evaluated **8p** (VU0476406) in both mouse and NHP models of L-DOPA-induced dyskinesia (LID), and found that administration of the M_4 PAM ameliorates deficits in synaptic plasticity and behavior in PD-LID mice and NHPs.[20] Specifically, **8p** dosed at 10 mg/kg IV (route chosen due to low cyno oral F, *vide supra*) significantly reduced dyskinesia scores and involuntary movements in NHPs, thus providing early proof-of-concept for M_4 PAMs in the management of Parkinson's disease and highlighting the utility of the compound **8p** (VU0476406) in NHP studies.

In summary, we have detailed the discovery and characterization of the first reported M_4 PAM non-human primate *in vivo* tool compound **8p** (VU0476406), with similar M_4 PAM activity across species. The studies presented here produced a required *in vivo* NHP POC tool compound for use in translational efficacy studies, primate PD models and biomarker studies that could be freely shared with collaborators. Initial results demonstrated that **8p** significantly reduces dyskinesia scores and involuntary movements in NHPs, and provided early POC for M_4 PAMs in the management of PD-LID. Further optimization efforts en route to M_4 PAM clinical candidates for the treatment of schizophrenia and other disorders will be reported in due course.

X-ray crystallographic data

The X-ray crystal structure data for **8p** was submitted to the Cambridge Crystallographic Data Centre (http://www.ccdc.cam.ac.uk) and assigned CCDC 1538487.

Acknowledgments

We thank the NIH for funding via the NIH Roadmap Initiative 1X01 MH077607 (C.M.N.), the Molecular Libraries Probe Center Network (U54MH084659 to C.W.L.), R01MH073676 (PJC) and U01MH087965 (Vanderbilt NCDDG). We also thank William K. Warren, Jr. and the William K. Warren Foundation who funded the William K. Warren, Jr. Chair in Medicine (to C.W.L.). We also thank key CROs that performed key higher species PK (Frontage), pharmaceutical science/X-ray work (Crystal Pharmatech) and Pgp assays (Absorption Systems).

References

1. Chan, W.Y.; McKinize, D.L.; Bose, S.; Mitchell, S.N.; Witkins, J.M.; Thompson, R.C.; Christopoulos, A.; Birdsall, N.J.; Bymaster, F.P.; Felder, C.C. *Proc. Natl. Acad. Sci. USA* **2008**, *105*, 10978-10983.
2. Leach, K.; Loiancono, R.E.; Felder, C.C.; McKinize, D.L.; Mogg, A.; Shaw, D.B.; Sexton, P.M.; Christopoulos, A. *Neuropsychopharmacology* **2010**, *35*, 855-869.
3. Brady, A.; Jones, C.K.; Bridges, T.M.; Kennedy, P.J.; Thompson, A.D.; Breininger, M.L.; Gentry, P.R.; Yin, H.; Jadhav, S.B.; Shirey, J.; Conn, P.J.; Lindsley, C.W. *J. Pharm. & Exp. Ther.* **2008**, *327*, 941-953.

4. Pancani, T.; Foster, D.J.; Bichell, T.; Bradley, E.; Bridges, T.M.; Klar, R.; Daniels, J.S.; Jones, C.K.; Bowman, A.B.; Lindsley, C.W.; Xiang, Z.; Conn, P.J. *Proc. Natl. Acad. Sci. USA,* **2015**, *112*, 14078-14083.
5. Foster, D.J.; Wilson, J.M.; Remke, D.H.; Mahmood, M.S.; Uddin, M.J.; Wess, J.; Patel, S.; Marnett, L.J.; Niswender, C.M.; Jones, C.K.; Xiang, Z.; Lindsley, C.W.; Rook, J.M.; Conn, P.J. *Neuron* **2016**, *91*, 1224-1252.
6. Byun, N.E.; Grannan, M.; Bubser, M.; Barry, R.L.; Thompson, A.; Rosanelli, J.; Gowrishnakar, R.; Kelm, N.D.; Damon, S.; Bridges, T.M.; Melancon, B.J.; Tarr, J.C.; Brogan, J.T.; Avison, M.J.; Deutch, A.Y.; Wess, J.; Wood, M.R.; Lindsley, C.W.; Gore, J.C.; Conn, P.J.; Jones C.K. *Neuropsychopharmacology* **2014**, *39*, 1578-1593.
7. Farrell, M.; Roth, B.L. *Neuropsychopharmacology* **2010**, *35*, 851-852.
8. Jones, C.K.; Byun, N.; Bubser, M. *Neuropsychopharmacology* **2012**, *37*, 16-42.
9. Shirey, J.K.; Xiang, Z.; Orton, D.; Brady, A.E.; Johnson, K.A.; Williams, R.; Ayala, J.E.; Rodriguez, A.L.; Wess, J.; Weaver, D.; Niswender, C.M.; Conn, P.J. *Nat. Chem. Bio.* **2008**, *4*, 42-50.
10. Le, U.; Melancon, B.J.; Bridges, T.M.; Utley, T.J.; Lamsal, A.; Vinson, P.N.; Sheffler, D.J.; Jones, C.K.; Morrison, R.; Wood, M.R.; Daniels, J.S.; Conn, P.J.; Niswender, C.M.; Lindsley, C.W. Hopkins, C.R. *Bioorg. Med. Chem. Lett.* **2013**, *23*, 346-350.
11. Kennedy, J.P.; Bridges, T.M.; Gentry, P.R.; Brogan, J.T.; Brady, A.E.; Shirey, J.K.; Jones, C.K.; Conn, P.J.; Lindsley, C.W. *ChemMedChem.* **2009**, *4*, 1600-1607.
12. Salovich, J.M.; Sheffler, D.J.; Vinson, P.N.; Lamsal, A.; Utley, T.J.; Blobaum, A.L.; Bridges, T.M.; Le, U.; Jones, C.K.; Wood, M.R.; Daniels, J.S.; Conn, P.J.; Niswender, C.M.; Lindsley, C.W.; Hopkins, C.R. *Bioorg. Med. Chem. Lett.* **2012**, *22*, 5084-5088.
11. Bubser, M.; Bridges, T.M.; Thorbeck, D.D.; Gould. R.W.; Grannan, M.; Noetzel, M.J.; Niswender, C.M.; Daniels, J.S.; Melancon, B.J.; Tarr, J.C.; Wess, J.; Duggan, M.E.; Brandon, N.J.; Dunlop, J.; Wood, M.W.; Wood, M.R.; Lindsley, C.W.; Conn, P.J.; Jones C.K. *ACS Chem. Neurosci.* **2014**, *5*, 920-942.
12. Smith, E.; Chase, P.; Niswender, C.M.; Conn, P.J.; Lindsley, C.W.; Madoux, F.; Acosta, M.; Scampavia, L.; Spicer, T.; Hodder, P. *J. Biomol. Screening* **2015**, *20*, 858-868.
13. Wood, M.R.; Noetzel, M.J.; Tarr, J.C.; Rodriguez, A.L.; Lamsal, A.; Chang, S.; Foster, J.J.; Smith, E.; Hodder, P.S.; Engers, D.W.; Niswender, C.M.; Brandon, N.J.; Wood, M.W.; Duggan, M.E.; Conn, P.J.; Bridges, T.M.; Lindsley, C.W. *Bioorg. Med. Chem. Lett.* **2016**, *26*, 4282-4286.
14. Wood, M.R.; Noetzel, M.J.; Engers, J.L.; Bollinger, K.A.; Melancon, B.J.; Tarr, J.C.; Han, C.; West, M.; Gregro, A.R.; Lamsal, A.; Chang, S.; Ajmera, S.; Smith, E.; Chase, P.; Hodder, P.S.; Bubser, M.; Jones, C.K.; Hopkins, C.R.; Emmitte, K.A.; Niswender, C.M.; Wood, M.W.; Duggan, M.E.; Conn, P.J..; Bridges, T.M.; Lindsley, C.W. *Bioorg. Med. Chem. Lett.* **2016**, *26*, 3029-3033.
15. Wood, M.R.; Noetzel, M.J.; Poslunsey, M.S.; Melancon, B.J.; Tarr, J.C.; Lamsal, A.; Chang, S.; Luscombe, V.B.; Weiner, R.L.; Cho, H.P.; Bubser, M.; Jones, C.K.; Niswender, C.M.; Wood, M.W.; Brandon, N.J.; Engers, D.W.; Duggan, M.E.; Conn, P.J.; Bridges, T.M.; Lindsley, C.W. *Bioorg. Med. Chem. Lett.* **2017**, *27*, 171-175.
16. Wood, M.R.; Noetzel, M.J.; Melancon, B.J.; Nance, K.D.; Poslunsey, M.S.; Hurtado, M.A.; Luscombe, V.B.; Weiner, R.L.; Rodriguez, A.L.; Lamsal, A.; Chang, S.; Bubser, M.; Blobaum, A.L.; Engers, D.W.; Niswender, C.M.; Jones, C.K.; Brandon, N.J.; Wood, M.W.; Duggan, M.E.; Conn, P.J.; Bridges, T.M.; Lindsley, C.W. *ACS Med. Chem. Lett.* **2017**, *8*, 233-238.
17. Experimental for the synthesis of **8p** (VU0476406), 5-amino-*N*-(4-(2-fluoropyridine-3-yl)benzyl)-3,4-dimethylthieno[2,3-*c*] pyridazine-6-carboxamide. To a 5 mL microwave vial equipped with a stir bar was added 5-amino-*N*-(4-bromobenzyl)-3-dimethylthieno[2,3-*c*]pyridazine6-carboxamide (50 mg, 0.13 mmol), (2-fluoropyridin-3-yl)boronic acid (36 mg, 0.26 mmol), 10 mol% Pd(dppf)Cl_2·CH_2Cl_2 (10.3 mg, 0.013 mmol). The microwave vial was sealed, evacuated and back-filled three times with argon. Then, an aqueous solution of potassium phosphate (380 μL, 1 M K_3PO_4 in H_2O, 0.38 mmol) was added, followed by THF (1.3 mL). The biphasic mixture was heated at 160 ^oC for 20 min, and after cooling, the suspension was diluted with DCM and filtered through celite. Silica gel chromatography afforded **8p** as an orange solid (40 mg, 80%). LCMS: R_T = 0.623 min, >99%@254 nm, >99%@215 nm; m/z (M+1) = 408. ^{1}H NMR (400 MHz, $CDCl_3$, d (ppm)): 8.7 (t, J=4.0 Hz, 1H), 8.2 (d, J=4.0 Hz, 1H), 8.1-8.0 (m, 1H), 7.6 (d, J=8.0 Hz, 2H), 7.5-7.4 (m, 3H), 6.9 (bs, 2H), 4.5 (d, J=4.0 Hz, 2H), 2.71 (s, 3H), 2.70 (s, 3H). HRMS calc'd for $C_{21}H_{19}FN_5OS$ (M+H), 408.1294; found 408.1298.
18. Whole and regional brain distribution of total and calculated unbound VU0476406 was determined in NHP (cynomolgus monkey, *n* = 1) via a PET study employing a single IV administration of [^{18}F]-VU0476406 (145 MBq) and an approximate 2 hour data acquisition time post-administration; manuscript in preparation.
19. Prediction of human CL_p was performed using two approaches: 1) the mean hepatic extraction ratio (ER_{hep}) observed in rat, dog, and NHP (0.17) applied to human Q_{hep}; 2) *in vitro* to *in vivo* extrapolation of CL_{int} (human hepatic microsomes) using the well-stirred model of organ clearance with inclusion of human fu_{plasma} and predicted fu_{mic} terms. Predicted human $t_{1/2}$ was obtained from predicted CL_p and a predicted V_{ss} (1.9 L/kg) scaled allometrically from the observed rat and dog V_{ss} with correction for species differences in fu_{plasma}.
20. Shen, W.; Plotkin, J.L.; Francardo, V.; Ko, W.K.D.; Xie, Z.; Li, Q.; Fieblinger, T.; Wess, J.; Neubig, R.R.; Lindsley, C.W.; Conn, P.J.; Greengrad, P.; Bezard, E.; Cenci, M.A.; Surmeier, D.J. *Neuron* **2015**, *88*, 762-773.